

# Using a Hybrid Laser Plus GMAW Process for Controlling the Bead Humping Defect

*The heat input from a defocused laser beam applied in front of a GMAW pool suppresses formation of weld bead hump defects and allows higher travel speeds*

BY H. W. CHOI, D. F. FARSON, AND M. H. CHO

**ABSTRACT.** A novel LBW + GMAW hybrid process was investigated, and its ability to suppress weld bead hump formation was characterized. The hybrid process had a relatively low-power-density laser spot focused a short distance in front of the leading edge of the GMA weld pool. The laser power and spot size were varied in tests and it was found that, for given GMAW process settings, bead humping was suppressed by laser heat input of sufficient power density. Comparison of the toe angles of humped and nonhumped weld beads made by the hybrid process and by the GMAW process suggested that capillary instability was likely a factor in weld bead hump formation, but it was not the sole factor in at least some of the tests. Observations made during the experiments suggested that weld pool fluid flows may have been an important factor in weld humping.

## Introduction

This article investigates a novel hybrid laser beam welding (LBW) plus gas metal arc welding (GMAW) process that provides for control of weld bead shape and suppression of the weld bead humping defect. Weld bead humping is a defect that often sets an upper limit on the travel speed that can be used with a welding process. Because of its importance, bead humping has been the subject of research for many years.

A first, relatively thorough qualitative study was reported by Bradstreet (Ref. 1). Humping was defined as a quasi-periodic weld bead shape defect that was always associated with undercutting; a failure of the molten weld deposit to completely fill a groove defined by the fusion boundary generated by arc heat input. Capillary or Rayleigh instability (Ref. 2) of the molten weld deposit due to liquid metal surface tension, wetting of the weld metal on the

adjacent solid substrate, and weld pool fluid flow were identified as factors important in hump formation, documented experimentally to various degrees and analyzed. Implicit in the discussions is the role of solidification since the humped geometry must be preserved by freezing the melt to be observed. It was noted that the hump defect was observed only at a high travel speed, that a leading ("push") weld gun travel angle suppressed hump formation, and oxygen in the shielding gas or from the weldment surface exacerbated hump formation.

Subsequent literature (Ref. 3) discussed these factors in more detail, offered some new ones (effect of gravity in uphill welding (Ref. 4)), and described how humping could be suppressed (e.g., two-electrode arc process (Ref. 5)). Marangoni flow was proposed as a factor in hump formation (Ref. 6) and was later noted as a relatively small effect in a paper dealing with the theoretical analysis of hump formation (Ref. 7). Studies aimed at understanding and controlling the bead humping phenomena through the adjustment of weld parameters and the dual torch welding approach continue to the present time (Refs. 8–10).

As high-energy electron beam (EB) and laser beam welding processes became important, a high-speed bead shape defect mode quite similar to arc weld bead humping was identified and analyzed (Refs. 11–16). Interestingly, the first archival article cited on this subject proposes a dual electron beam solution to the

problem. Because the high-energy-density processes are inherently high speed and produce narrow deep welds, weld metal flow is generally identified as being more important in humping than surface tension. Although the deep narrow welds associated with high-energy-density processes are not the same as the GMA weld bead of interest in this work, it is interesting that the dual heat source strategy for weld humping suppression was not adopted in arc welding and laser beam welding (Refs. 17, 18) until some years later. A novel humping suppression method for laser welding that is based on Lorentz force exerted by a current flow specifically introduced for this purpose has been demonstrated (Ref. 19).

One can conclude from the above cited literature that two factors are identified as dominant causes of the humping defect in arc weld beads. Both were mentioned in the seminal work by Bradstreet. Capillary instability is one key factor that is emphasized in that work, and also in the overview and theoretical analysis by Kapadia and Dowden. However, longitudinal flow in the weld pool, which becomes faster as travel speed and corresponding wire deposition rate increases for filler-added processes, is a second factor that is commonly identified.

Bradstreet identified a submerged flow stream that originates from the bottom of the weld pool crater and sweeps backward along the centerline solidification boundary to the trailing edge of the pool. Two other rearward-directed streams originate higher up on either side of the crater and merge with the centerline flow somewhere between the crater and the trailing edge of the weld pool. At this point, the longitudinal flow, which has been attenuated from energy removal due to solidification, emerges on the melt surface and sometimes is seen moving relatively sluggishly toward the leading edge of the pool as a surface flow. Nguyen et al. (Ref. 8) noted these same flows in high-speed photographs and identified them as the dominant cause of humping in his welds.

For arc welding processes, most of the

## KEYWORDS

Laser Beam Welding (LBW)  
Gas Metal Arc Welding (GMAW)  
Weld Bead Humping  
Hybrid Process  
Bead-on-Plate Welds  
Capillary Instability

H. W. CHOI, D. F. FARSON (farson.4@osu.edu), and M. H. CHO are with The Ohio State University, Welding Engineering Program, Columbus, Ohio.

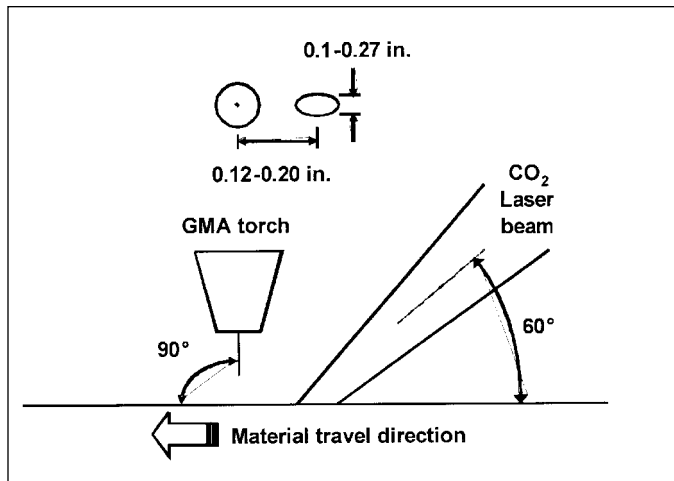


Fig. 1 — Hybrid process setup.

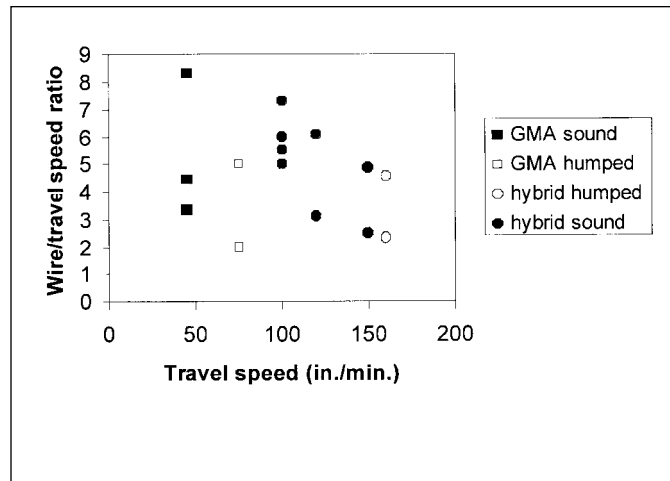


Fig. 2 — Travel speed limits of the GMAW and hybrid processes for bead-on-plate welds. Sound (nonhumped) weld beads were not possible at 80 in./min with the GMAW process, but were possible at 150 in./min (3.75 m/min) and with a higher deposition rate with the hybrid process.

**Table 1 — Welding Apparatus and Process Settings**

GMAW power source	ESAB Dipipulse 450i cvcc
GMAW pulse mode/trim	Synergic/99-122
Filler material/diameter	ER70S-6/0.045 in. (1.1 mm)
Base material/thickness	HR 1008 steel plate/14, 16 gauge
Shielding gas/flow rate	Ar, 90% Ar-10% CO <sub>2</sub> / 35 ft <sup>3</sup> /h (14 L/min)
Contact tip-to-work distance	0.875 in. (22 mm)
Laser	Rofin Sinar RS850
Laser focus optic/focal length	Parabolic mirror/10 in. (25.4 mm)
Laser focus spot width W <sub>1</sub>	0.1–0.27 in. (2.54–6.86 mm)
Laser power P <sub>1</sub>	2.0–3.5 kW
Arc laser spot spacing	0.13–0.2 in. (3–5 mm)

research literature deals with the bead-on-plate weld geometry. No literature can be found for bead humping in the more useful lap-fillet and T-fillet groove geometries. For this research, it is also interesting that dual-torch processes have been found to be less susceptible to hump formation than single-torch processes.

Independent of the welding applications research into weld bead humping, closely related, but more fundamental, studies into wetting and spreading (both isothermal and nonisothermal) of liquid and solid substrates have been proceeding. Dynamic nonisothermal wetting and spreading of a linear “bead” of liquid deposited on a solid surface has been analyzed and conditions for instability (essentially, capillary-force driven instability) were determined (Ref. 20).

Even more pertinent to welding, a nonisothermal analysis of a similar situation that allows for heat transfer and solidification of the liquid has also been carried out (Ref. 21). In this work, it is reported that liquid deposits that are well wetted to the substrate (i.e., have an internally measured contact angle of less than  $\pi/2$ ) are not susceptible to humping by capillary in-

stability. This result is in agreement with the earlier isothermal analysis.

Another key result from nonisothermal wetting analysis is that melt spreading speed is controlled by surface energies and resulting contact angle, very much as in an isothermal wetting case. However, the maximum extent of nonisothermal spreading is ultimately limited by heat transfer and phase transformation; simply put, when the metal freezes, it ceases to spread. This is a key insight that is useful when configuring laser heat input so as to produce desired weld bead shapes.

In this article, we return to the original concept of humping as a capillary instability for inspiration that suggests a new technique that may permit control of the defect. We propose that a defocused laser beam can be used as an auxiliary heat source to control the shape of the deposited weld metal. In the experiments described in this article, the laser beam is defocused into a relatively broad spot that travels with the arc and is directed onto the weldment in advance of the leading edge of the weld pool.

It is hoped that this additional surface heat input will heat and melt a shallow,

broad area that will allow the molten weld metal to spread laterally, decreasing the toe angle and thereby decreasing the capillary instability of the molten deposit. The ability to adjust this additional heat source so as to prevent weld bead humping is characterized, and its effects are analyzed. In particular, the effects of capillary forces and flow on weld bead humping are deduced from the experimental results.

## Experimental Apparatus and Procedure

A GMAW apparatus that allowed for flexible integration of a laser beam heat source was integrated. A sketch of the position and orientation of the GMAW process and laser beam focus is shown in Fig. 1, and details of the welding process settings are given in Table 1. A pulsed GMAW power source was used to deposit bead-on-plate welds in the flat position on hot-rolled steel sheet with as-received surface condition. With the exception of wire feed and travel speed, the GMAW process settings remained fixed during all tests. The laser beam focus spot was positioned in front of the leading edge of the GMAW weld pool, and the focal point elevation was adjusted to produce a laser focus spot diameter measured normal to the travel direction.

Relative positions and orientations of the arc and laser processes and other welding process variable settings are summarized in Fig. 1. The laser beam incidence angle setting remained fixed during the tests, and the relative position of the laser spot and the arc were fixed at 0.1–0.2 in. (0.25–0.5 mm). However, the laser power and focus spot size were varied to determine their effects on hump preven-

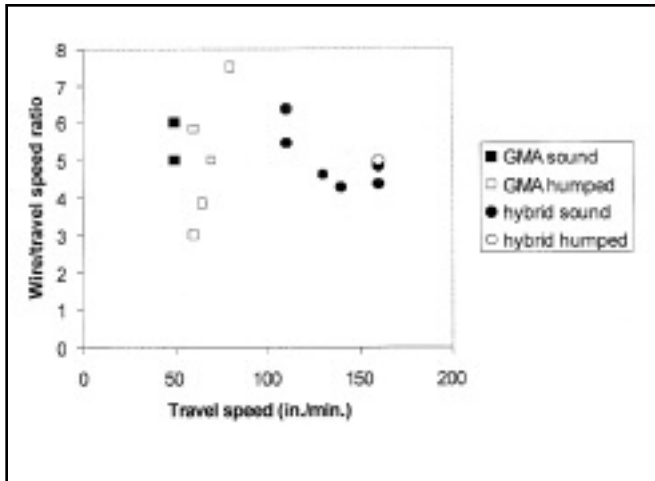


Fig. 3 — Travel speed limits of the GMAW and hybrid processes for lap-fillet welds. Sound (nonhumped) weld beads were not possible at 60 in./min with the GMAW process, but were possible at 160 in./min (4 m/min) and with a higher deposition rate with the hybrid process. 160 in./min (4 m/min) was the maximum travel speed of the motion system.

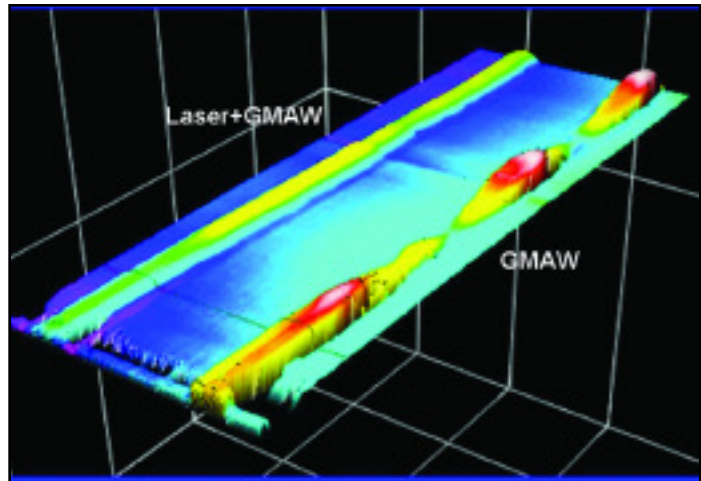


Fig. 4 — Surface contour images of a GMAW-only weld with hump defects and hybrid process weld with desired weld bead shape. Travel speed was 80 in./min (2 m/min), and GMAW process settings were the same in both cases.

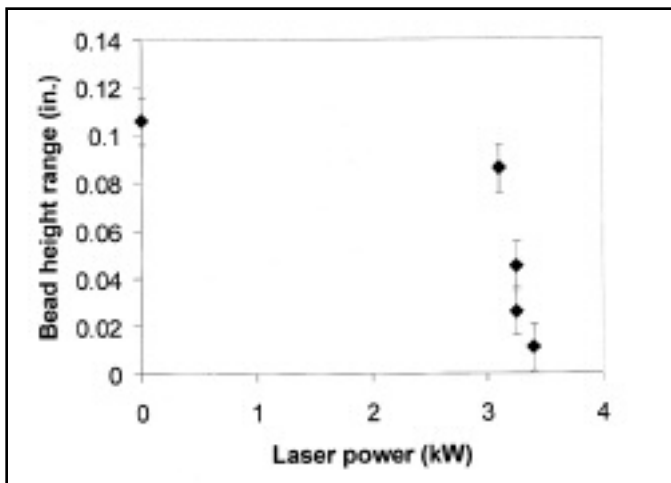


Fig. 5 — Variation of BOP weld bead hump height variation as a function of laser power for conditions  $W_L = 0.2$  in. (5 mm), Ar shielding gas, 14-gauge material.

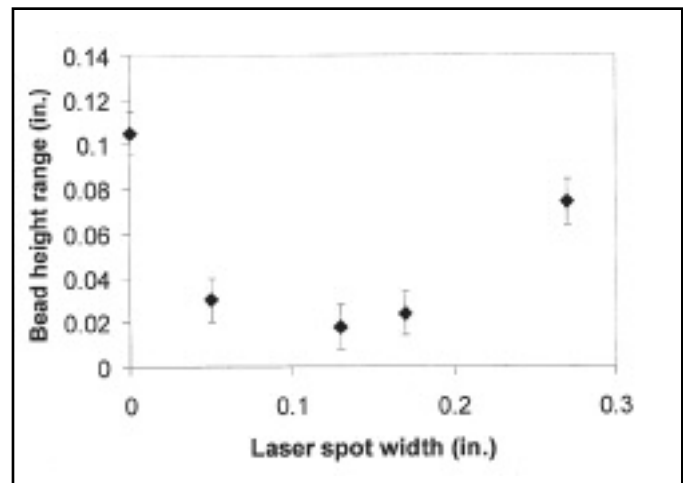


Fig. 6 — Variation of BOP weld bead hump height variation as a function of laser spot width for conditions Ar+10%CO<sub>2</sub> shielding gas, 14-gauge material. Laser power was not constant for the tests.

tion. Argon was used as a shielding gas for some initial tests because it is known to exacerbate weld bead humping. However, as more experience was gained with the bead humping defect, it was found that humping was obtained at feasible travel speeds with the more conventional 90% argon-10% CO<sub>2</sub> shielding gas, which was used for the majority of the tests. After welding, the standard deviation and range (maximum–minimum) of the height and the weld toe angles of the bead-on-plate welds were measured using a laser line scan weld inspection system (Servo-Robot WISC).

## Experimental Results

Hybrid and GMA bead-on-plate welds were made over a range of wire feed

speed, travel speed, and other process variable settings. Bead humping severity was quantified by measuring the range of weld bead height over the length of the weld, and the effect of various process settings on bead height variation was determined. Laser beam heating was found to suppress weld bead humping in both bead-on-plate (Fig. 2) and lap-fillet (Fig. 3) weld geometries. These figures show that for comparable deposit areas, the hybrid process was able to operate at a higher travel speed without bead humping — the speed for acceptable (nonhumped) bead-on-plate and lap-fillet welds was nearly a factor of two higher for the hybrid process. However, it is also interesting to note that beads deposited with the hybrid process also formed humps when the travel speed

was sufficiently large. Humped beads were defined as those having a bead height variation along their length more than 0.03 in. (0.75 mm).

A graphical illustration of the hump prevention capability of the hybrid process is shown in Fig. 4. Two bead-on-plate welds made with the same GMAW settings are shown — the one made with the hybrid process has a smooth contour, while the other made with the GMAW process alone is severely humped.

The bead-on-plate welds were studied in more detail to determine parameter effects on humping. The experimental results are compiled in Table 1, and the effects of laser power and laser spot size weld bead humping are quantified in Figs. 5 and 6. For these tests, the conditions

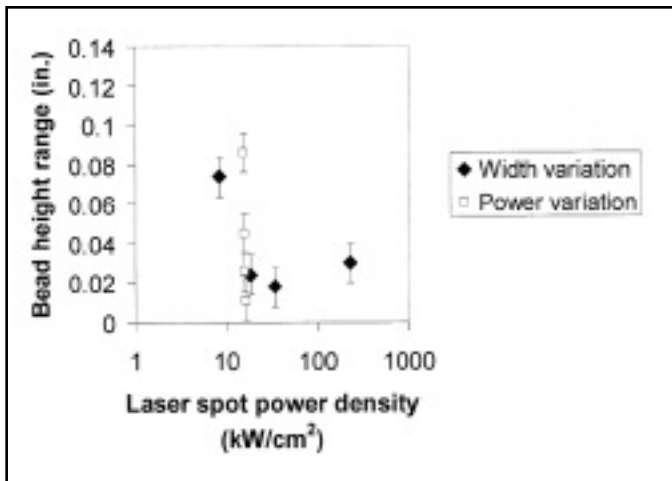


Fig. 7 — Variation of BOP weld bead hump height variation as a function of laser power spot density from Figs. 5 and 6. A threshold power density of about 16 kW/cm<sup>2</sup> is observed.

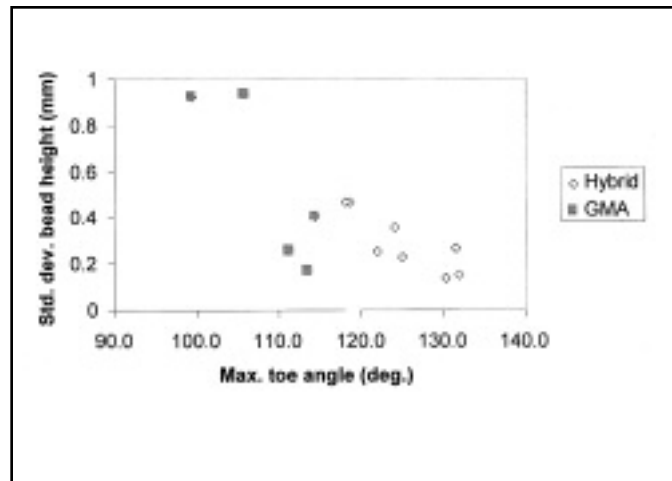


Fig. 8 — Weld bead height variation vs. maximum toe angle for argon shielding gas and varying process settings. The hybrid welds generally had larger toe angles and were of comparable smoothness to GMA welds.

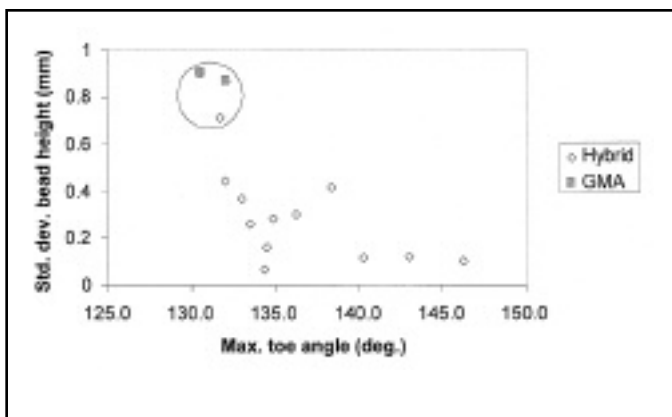


Fig. 9 — Weld bead height variation vs. maximum toe angle for CO<sub>2</sub> shielding gas and varying process settings. The hybrid welds generally had larger toe angles and were smoother than GMA welds. Hybrid and GMA welds with comparable angles are marked.

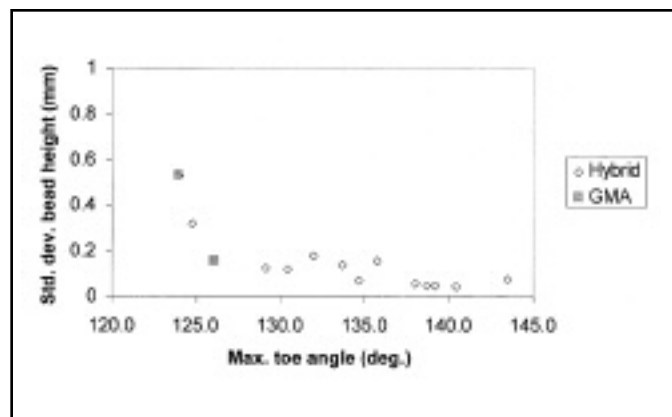


Fig. 10 — Weld bead height variation vs. maximum toe angle for 16-gauge material and varying process settings. The hybrid welds generally had larger toe angles and were smoother than GMA welds.

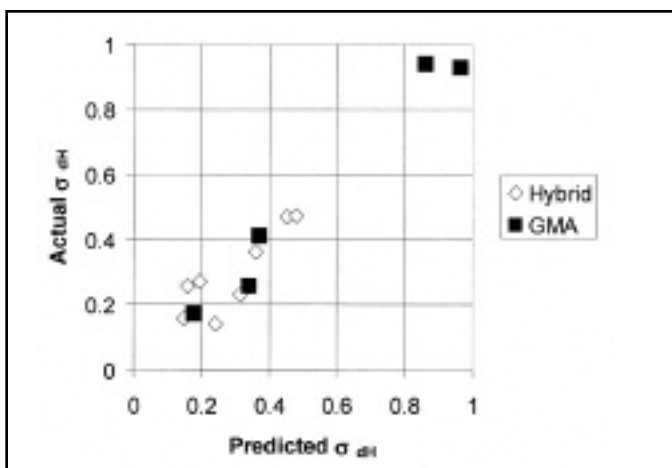


Fig. 11 — Actual standard deviation of weld bead height ( $\sigma_{6h}$ ) compared to the standard deviation predicted by a linear regression equation with inputs of laser power, travel speed, wire feed speed, and maximum toe angle for the 12-gauge argon welds. The correlation coefficient was  $R^2 = 0.94$ , indicating that the linear combination of these variables explained most of the bead humping in these experiments.

were  $S = 100$  in./min (42 mm/s) and  $S_w = 550$  in./min (233 mm/s). For a fixed laser spot size of 0.2 in. (0.5 mm), a power of slightly more than 3 kW was needed to suppress humping. Laser spot widths of 0.05 in. (1.3 mm) or more were found to suppress humping, but the widest spot of 0.27 in. (6.9 mm) did not. Since laser power was adjusted during the tests depicted in Fig. 6 to maintain comparable power den-

sities, the results from Figs. 5 and 6 are plotted against laser power density in Fig. 7. These results show that irrespective of width or power variation, a laser power density of approximately 16 kW/cm<sup>2</sup> was sufficient to suppress bead humping. Also, it was noticed that the power density of the widest spot from Fig. 6 was only about 8 kW/cm<sup>2</sup>, which is less than the threshold needed to prevent humping.

This research was initiated with a hypothesis that the GMAW humping defect could be prevented by adding additional heat sources to the welding process to promote wider weld beads with smaller internal wetting angles (equivalently, larger external toe angles), thereby avoiding capillary instability. To test whether the observed humping suppression was due to this effect, toe angles (external angles measured by laser scanner) were compared to the critical angle of 90 deg for various welding conditions. Note that the

**Table 2 — Experimental Conditions and Results**

Condition	S <sub>w</sub> in./min	S in./min	P <sub>l</sub> kW	W <sub>l</sub> in.	Range dH in.	σ <sub>dH</sub> Standard Deviation dH mm	θ <sub>m</sub> Max. Toe Angle (deg)
12 gauge, Argon	500	80	0	0	0.044	0.411	114.3
	500	70	0	0	0.017	0.259	111.2
	500	60	0	0	0.018	0.174	113.5
	500	80	3	0.1	0.01	0.257	121.9
	500	100	3	0.1	0.03	0.471	118.6
	550	100	3.35	0.21	0.068	0.473	118.1
	550	100	3.35	0.2	0.016	0.158	131.9
	600	100	3.35	0.2	0.08	0.363	124.0
	630	100	3.35	0.2	0.021	0.271	131.4
	550	100	3.1	0.2	0.086	0.916	122.6
	550	100	3.25	0.2	0.045	1.413	123.2
	550	100	3.25	0.2	0.026	0.364	125.0
	550	100	0	0.2	0.106	0.926	99.3
	550	100	3.4	0.2	0.011	0.232	125.0
	680	100	3.35	0.2	0.025	0.142	130.3
	680	100	0	0	0.121	0.938	105.7
12 gauge, Ar+CO <sub>2</sub>	600	100	0	0	0.101	0.904	130.5
	600	100	3.35	0.2	0.101	0.068	134.4
	600	100	3.35	0.2	0.022	0.259	133.5
	650	100	3.1	0.2	0.013	0.104	146.3
	650	100	3.1	0.2	0.008	0.446	132.0
	600	100	3.3	0.2	0.03	0.713	131.7
	600	100	3.35	0.05	0.018	0.284	134.8
	600	100	3.55	0.13	0.074	0.419	138.3
	600	100	0	0.17	0.105	0.869	132.0
	650	100	3.35	0	0.145	0.12	143.0
	700	100	3.35	0.188	0.1525	0.115	140.3
	650	100	3	0.178	0.1545	0.37	133.0
	650	100	3.25	0.26	0.143	0.301	136.2
	650	100	3.5	0.26	0.156	0.163	134.5
16 gauge, Ar+CO <sub>2</sub>	500	100	0	0	0.063	0.53	123.9
	500	100	2.5	0.167	0.005	0.157	135.7
	300	100	2	0.15	0.013	0.075	143.4
	300	100	0	0	0.058	0.157	126.0
	300	130	2	0.15	0.005	0.141	133.6
	300	150	2	0.15	0.013	0.324	124.8
	375	150	2	0.15	0.006	0.126	129.1
	375	120	2	0.17	0.003	0.044	140.4
	350	100	2	0.2	0.011	0.051	138.6
	375	150	2	0.16	0.016	0.182	131.9
	375	120	2	0.16	0.005	0.051	139.1
	450	140	2	0.162	0.007	0.12	130.4
	440	130	2	0.16	0.005	0.072	134.6
	400	130	2	0.16	0.005	0.056	138.0

S<sub>w</sub>: wire feed speed; S: travel speed; P<sub>l</sub>: laser power; W<sub>l</sub>: laser spot width; σ<sub>dH</sub>: standard deviation of weld bead height variation; θ<sub>m</sub>: maximum weld toe angle.

maximum toe angle is used based on a supposition that the stability of an asymmetrical weld deposit should be controlled by the larger of the two toe angles.

The results, summarized in Figs. 8–10 for noted conditions, show that the laser hybrid welds did indeed have larger toe angles and less height variations as quantified by the standard deviation of weld bead height over the length of the weld. However, there is considerable scatter in the correlation between the two variables. This variability is due to the fact that the points in Figs. 8 and 9 represent many different GMA and hybrid process settings. It is also notable that all of the measured

toe angles are significantly greater than the critical static angle of 90 deg. In itself, this indicates that factors besides capillary instability play a role in the bead hump formation in our experiments.

To quantify the role played by other welding parameters in the toe angle-bead humping relationship, a multilinear regression was carried out on the data of Fig. 8. The result was a linear equation of the form

$$\sigma_{dH} = -0.024\theta_m + 0.011S - 0.0004S_w - 0.010P_l + 2.056 \quad (1)$$

where the symbols are as defined in Table 2. The predictions of the equation are compared to the actual weld bead height standard deviation in Fig. 11. The data were relatively well fit by the linear combination of these variables, with a correlation coefficient of R<sup>2</sup> = 0.94. The sign of the coefficients indicates that larger maximum toe angle and laser power decreased bead height variation, while higher travel speed and wire feed speed increased it. When a regression was done with coded variables so that coefficients could be easily compared, it was found that they were all of the same order of magnitude, indicating that the contribution of process settings to the bead humping was comparable to the toe angle. It is noted that linear regression fitting of the data of Figs. 9 and 10 produced correlation coefficients of R<sup>2</sup> = 0.77 and R<sup>2</sup> = 0.68, suggesting that a model with higher order terms would be needed to more accurately represent the data.

Further analysis showed more vividly that hump formation is sometimes affected by factors other than capillary instability. All other process settings being equal, additional laser heat input would inevitably result in a longer weld pool and more time for capillary instability to form a humped weld bead. Thus, for the same weld toe angle and GMA process settings, it might be expected that bead height variation of the hybrid weld beads would probably be worse than GMA weld beads if capillary forces were the sole factor in humping. However, several data points for this case (three points on the left side of Fig. 9; data are highlighted in Table 2) show that a hybrid weld with the same toe angles as GMA welds was humped less. Thus, it may be concluded that the beneficial effects of the hybrid process were not solely due to improved weld bead shape.

A likely additional effect of the hybrid process was noticed while doing the experiments — it was observed that the leading edge of the weld pool was located further in advance of the welding arc for the hybrid process when laser power was high enough to be effective. This change would significantly effect weld pool fluid flow by decreasing the conversion of downward droplet momentum into backward weld pool jet momentum. Considering this affect, it is conjectured that the mechanism of humping suppression of the hybrid process investigated in this work may be similar to that of the two-arc or dual-beam processes mentioned in the literature survey.

## Conclusions

A novel LBW plus GMAW hybrid process was investigated, and its ability to suppress weld bead hump formation was

characterized. It was found that, for given GMAW process settings, bead humping was suppressed by laser heat input of sufficient power density. Comparison of the aspect ratios of humped and nonhumped weld beads made by the hybrid process and by the GMAW process suggested that capillary instability was not the only factor in bead humping. Observations made during the experiments suggested that weld pool fluid flows were also important.

### References

1. Bradstreet, B. J. 1968. Effect of surface tension and metal flow on weld bead formation. *Welding Journal* 47(7): 314-s to 322-s.
2. Rayleigh, J. W. S. 1892. On the stability of cylindrical fluid surfaces. *Phil. Mag.* 5(34): 177-180.
3. Savage, W. F., Nippes, E. F., and Agusa, K. 1979. Effect of arc force on defect formation in GTA welding. *Welding Journal* 58(7): 212-s to 224-s.
4. Scotti, A., Larson, U., and Norrish, J. 1991. Bead instability of mechanised P-MIG [pulsed MIG] welding in vertical-up position. *Int. J. Joining Mater.* 3(1): 18-24.
5. Kokura, S., Nihei, M., Kozono, U., Ashida, E., and Onuma, A. 1980. Twin electrode switching arc welding method. Report 1: High speed twin electrode switching TIG welding. *J. Japan Weld. Soc.* 49(4): 259-265.
6. Mills, K. C., and Keene, B. J. 1990. Factors affecting variable weld penetration. *Int. Mater. Rev.* 35: 185-216.
7. Gratzke, U., Kapadia, P. D., Dowden, J., Kroos, J., and Simon, J. 1992. Theoretical approach to the humping phenomenon in welding processes. *J. Phys. D: Appl. Phys.* 25(11): 1640-1647.
8. Nguyen, T. C., Weckman, D. C., Johnson, D. A., and Kerr, H. W. 2005. The humping phenomenon during high speed gas metal arc welding. *Sci. Technol. Welding Joining* 10(4): 447-459.
9. Mendez, P. F., and Eagar, T. W. 2003. Penetration and defect formation in high-current arc welding. *Welding Journal* 82(10): 296-s to 306-s.
10. Ueyama, T., and Ohnawa, T. 2005. Effects of torch configuration and welding current on weld bead formation in high speed tandem pulsed gas metal arc welding of steel sheets. *Sci. Technol. Welding Joining* 10(6): 750-759.
11. Arata, Y., and Nabegata, E. 1978. Tandem Electron Beam Welding (Report 1). *Trans. JWRI* 7(10): 101-109.
12. Tsukamoto, S., Irie, H., Inagaki, M., and Hashimoto, T. 1982. Humping bead formation in electron beam welding. Report 2: Effect of beam current on humping bead formation. *J. Japan Welding Soc.* 51(10): 867-873.
13. Tsukamoto, S., Irie, H., Inagaki, M., and Hashimoto, T. 1983. Effect of focal position on humping bead formation in electron beam welding. *Trans. Nat. Res. Inst. Metals* 25(2): 62-67.
14. Tsukamoto, S., Irie, H., Inagaki, M., and Hashimoto, T. 1984. Effect of beam current on humping bead formation in electron beam welding. *Trans. Nat. Res. Inst. Metals* 26(2): 133-140.
15. Tomie, M., Abe, N., and Arata, Y. 1989. Tandem electron beam welding. Report 9: High speed tandem electron beam welding. *Trans. JWRI* 18(2): 175-180.
16. Albright, C. S., and Chiang, S. 1988. High speed laser welding discontinuities. *J. Laser Applications* 1(1): 18-24.
17. Iwase, T., Sakamoto, H., Shibata, K., Hohenberger, B., and Dausinger, F. 2000. Dual focus technique for high-power Nd:YAG laser welding of aluminum alloys. *Proc SPIE* 3888: 348-358.
18. Xie, J. 2002. Dual beam laser welding. *Welding Journal* 81(10): 223-s to 230-s.
19. Kern, M., Berger, P., and Hugel, H. 2000. Magneto-fluid dynamic control of seam quality in CO<sub>2</sub> laser beam welding. *Welding Journal* 79(3): 72-s to 78-s.
20. Davis, S. H. 1980. Moving contact lines and rivulet instabilities. Part 1. The static rivulet. *J. Fluid Mech.* 98: 225-242.
21. Schiaffino, S., and Sonin, A. A. 1997. Formation and stability of liquid and molten beads on a solid surface. *J. Fluid Mech.* 343: 95-110.

## Preparation of Manuscripts for Submission to the *Welding Journal* Research Supplement

All authors should address themselves to the following questions when writing papers for submission to the *Welding Research Supplement*:

- ◆ Why was the work done?
- ◆ What was done?
- ◆ What was found?
- ◆ What is the significance of your results?
- ◆ What are your most important conclusions?

With those questions in mind, most authors can logically organize their material along the following lines, using suitable headings and subheadings to divide the paper.

- 1) **Abstract.** A concise summary of the major elements of the presentation, not exceeding 200 words, to help the reader decide if the information is for him or her.
- 2) **Introduction.** A short statement giving relevant background, purpose, and scope to help orient the reader. Do not duplicate the abstract.
- 3) **Experimental Procedure, Materials, Equipment.**
- 4) **Results, Discussion.** The facts or data obtained and their evaluation.
- 5) **Conclusion.** An evaluation and interpretation of your results. Most often, this is what the readers remember.

### 6) Acknowledgment, References and Appendix.

Keep in mind that proper use of terms, abbreviations, and symbols are important considerations in processing a manuscript for publication. For welding terminology, the *Welding Journal* adheres to AWS A3.0:2001, *Standard Welding Terms and Definitions*.

Papers submitted for consideration in the *Welding Research Supplement* are required to undergo Peer Review before acceptance for publication. Submit an original and one copy (double-spaced, with 1-in. margins on 8 ½ x 11-in. or A4 paper) of the manuscript. A manuscript submission form should accompany the manuscript.

Tables and figures should be separate from the manuscript copy and only high-quality figures will be published. Figures should be original line art or glossy photos. Special instructions are required if figures are submitted by electronic means. To receive complete instructions and the manuscript submission form, please contact the Peer Review Coordinator, Erin Adams, at (305) 443-9353, ext. 275; FAX 305-443-7404; or write to the American Welding Society, 550 NW LeJeune Rd., Miami, FL 33126.